First Study of Heavy-Ion Mirror Charge Exchange

M. Steiner, Sam M. Austin, D. Bazin, W. Benenson, C. A. Bertulani,* J. A. Brown, M. Fauerbach, M. Hellström,† E. Kashy, J. H. Kelley, R. A. Kryger, T. Kubo,‡ N. A. Orr,§ R. Pfaff, B. M. Sherrill, M. Thoennessen, S. J. Yennello,‖ B. M. Young,¶ and P. D. Zecher

National Superconducting Cyclotron Laboratory and Department of Physics and Astronomy, Michigan State University, East Lansing, Michigan 48824-1321

D. J. Morrissey and C. F. Powell

National Superconducting Cyclotron Laboratory and Department of Chemistry, Michigan State University, East Lansing, Michigan 48824-1321

(Received 3 August 1995)

Differential cross sections have been measured near 0° for the dominant channels in the mirror reaction ^{13}C(^{13}N,^{13}C)^{13}N at $E/A = 57$ and 105 MeV. The cross sections of the peaks in the excitation spectrum are discussed in terms of Gamow-Teller and Fermi transition strength. The cross section per unit Gamow-Teller strength is found to be enhanced relative to that for unit Fermi strength when compared with previous results from (p,n) reactions. The present work represents the first use of a mirror-symmetric projectile and target system in a charge-exchange reaction as well as the first application of the developing radioactive nuclear beam field to this area.

PACS numbers: 25.70.Kk, 24.30.Cz, 25.60.Lg, 27.20.+n

Recent developments in the rapidly growing field of radioactive nuclear beams (RNB) have opened up new areas of research, and RNBs are expected to help answer a number of important questions in nuclear physics. Experiments with a wide variety of radioactive nuclei, many of them of astrophysical importance, have become possible, and exciting new phenomena are being observed.

Among the new capabilities provided by RNBs are nuclear reaction studies with mirror nuclear pairs, since only one member of a mirror pair can be stable. Because of their special symmetry, mirror pairs are useful tools for the study of the strong force in a nuclear environment, and they provide a unique opportunity for attaining the long-term goal of understanding charge exchange in heavy ions. In the present work, we study the relative importance of spin-flip and non-spin-flip contributions to heavy-ion charge exchange (HICEX) and investigate the usefulness of this reaction for determining Gamow-Teller (GT) transition strengths in nuclei. Weak-interaction strengths are of fundamental interest for our understanding of the nucleus, and GT matrix elements are important input parameters in nuclear astrophysics calculations for a large number of radioactive nuclei [1].

The most direct measurements of GT transition strengths, B(GT), are obtained from allowed β decay, but are limited by the small accessible excitation energy range. Charge-exchange (p,n) reactions at energies above 100 MeV have long been used to measure GT strengths over a wide range of excitation energies, and a well-established relationship exists between the forward cross section $d\sigma/d\Omega(0°)$ and B(GT) [2,3]. This latter method can in principle also be used for unstable nuclei by means of inverse-kinematics experiments with radioactive beams on hydrogen targets. If good energy resolution is to be obtained, however, these experiments will be difficult, since they involve the detection of rather low-energy neutrons. Furthermore, experiments in the β^+ direction are not possible, since there are no neutron targets.

Heavy-ion charge exchange has the potential to become a powerful tool for GT strength measurements if a reliable calibration analogous to that in the (p,n) case can be found or, more desirably, if the reaction mechanism and its relation to GT strength can be understood in detail. HICEX offers favorable kinematics, the capability to sample both the β^+ and β^- directions, and the additional advantage of quantum selectivity for certain projectile-ejectile choices. In the (^{6}Li,^{6}He) reaction, for example, final states can be chosen that limit the transitions to $\Delta S = 1, \Delta T = 1$ [4]. Experimental efforts with stable beams have relied on calibration to known GT transitions for the extraction of new information in the same nucleus and have found a good correlation between forward cross section and transition strength [4–6]. By studying reaction products around 0°, small linear and angular momentum transfers are favored. Contributions from the competing process of sequential stripping and pickup of nucleons are estimated from a systematic study of the ^{12}C(^{12}C,^{12}N)^{12}B reaction, where GT strengths are comparable, to be approximately 30% near 60 MeV and negligible at $E/A \geq 100$ MeV [7]. Based on the work outlined in Refs. [5,8], further complications that arise from the structure and finite size of the projectile are expected to be of little importance in the present situation. Elastic and inelastic scattering at backward angles, which contributes coherently to charge exchange, is negligible due to the strong absorption (see, e.g., Ref. [9]).

Two ^{13}C(^{13}N,^{13}C)^{13}N experiments were performed at the MSU NSCL radioactive-beam facility with secondary-

 0031-9007/96/76(1)/26(4)$06.00

beam energies per nucleon of 57 and 105 MeV. The A1200 fragment separator was used in a dispersion-matched mode [10], achieving an energy resolution (FWHM) of 1 MeV (1.5 MeV) at $E/A = 57$ MeV (105 MeV) despite an energy spread of the secondary beam of approximately 15 MeV (27 MeV). Detailed experimental parameters are given in Table I. The primary ^{14}N beam impinged on a thick ^{9}Be target, producing projectile fragments with near-beam velocities. The first A1200 dipole stage was set to select ^{13}N ions, collimate them, and focus them onto a thin ^{13}C-labeled polyethylene target located at a dispersive intermediate image. The ^{13}C reaction products were focused by the second dipole stage onto the A1200 focal plane, which consisted of two two-dimensional position-sensitive drift chambers, a position-sensitive silicon detector, and a large plastic scintillator. Positions and angles as well as time-of-flight, energy loss, and total-energy signals were recorded for each ion. Particle trajectories measured at the focal plane were converted into scattering angles at the reaction target, and angular distributions were obtained for the secondary beam as well as the reaction products. Using ^{13}N as a test beam, trajectories at the reaction target and the focal plane were recorded simultaneously, and the ion-optical parameters of the A1200 were determined. The excitation energy was measured by means of the momentum dispersion of the ^{13}C nuclei at the focal plane. ^{13}N ions exiting the reaction target in the $6+$ charge state had magnetic rigidities very close to the ^{13}C reaction products and provided a convenient energy calibration. The $^{13}N^{6+}/^{13}N^{7+}$ charge state ratio was experimentally determined at the two energies (see Table I), and the $^{13}N^{6+}$ rate was used to monitor the secondary-beam intensity.

Figures 1 and 2 show the focal-plane position spectra recorded simultaneously for the $^{13}N^{6+}$ charge state and the $(^{13}\mathrm{N}, ^{13}\mathrm{C})$ reaction products at $E/A = 57$ and 105 MeV, respectively. The slight shift and larger width of the ^{13}C ground state (g.s.) peak compared to $^{13}N^{6+}$ is due to differential energy loss in the reaction target. The peaks in (p, n) spectra can be readily associated with states in the target nucleus, but the present situation is complicated by

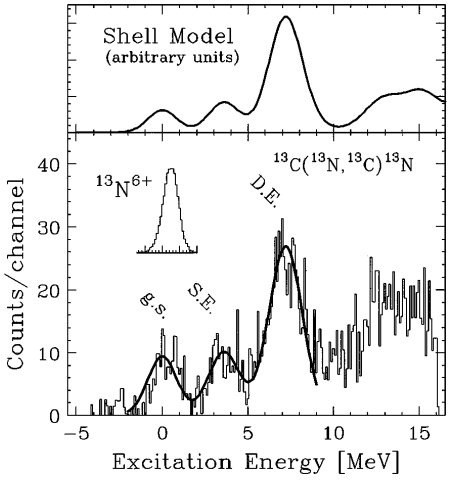

FIG. 1. $^{13}\mathrm{C}(^{13}\mathrm{N}, ^{13}\mathrm{C})^{13}\mathrm{N}$ energy spectrum at $E/A = 57$ MeV. The top curve is a calculation using the experimentally obtained σ^* values and shell-model GT strengths [11], scaled by the conventional quenching factor of 0.67 [11] and convoluted with the experimental resolution. The curve closely resembles the general shape of the experimental data (bottom) over the accessible excitation-energy range. The bottom curve is a fit to the data with the peak heights as free parameters and is used in determining the cross sections. The inset shows the $^{13}N^{6+}$ secondary-beam charge state, observed simultaneously.

the fact that both target and projectile can be excited. In the following discussion, we will concentrate on the two lowest-lying negative-parity states in the $A = 13$ mirror pair: the $J^\pi = 1/2^-$ ground state and the $3/2^-$ excited state at 3.68 MeV (3.50 MeV for ^{13}N). These are the only states below 10 MeV that are strongly excited by charge-exchange reactions in this energy region [12], and they dominate the low-energy part of the spectrum. The peaks in Figs. 1 and 2 are identified as follows: (a) g.s., both ejectile and target residue are in their ground states; (b) single excitation (SE), the target residue is in the $1/2^-$ ground state and the ejectile in the $3/2^-$ state, or vice versa; and (c) double excitation (DE), both nuclei are in the $3/2^-$ state. The unresolved structure above 10 MeV excitation energy represents GT transitions to a number of negative-

TABLE I. Experimental parameters and results for the mirror charge-exchange experiments.

^{13}N energy	$E/A = 57$ MeV	$E/A = 105$ MeV
Intensity (approx.)	5×10^6 s^{-1}	6×10^5 s^{-1}
Reaction target	^{13}C, 9.0 mg/cm^2	^{13}C, 18.0 mg/cm^2
^{13}C resolution	2.0 MeV	2.4 MeV
$^{13}N^{6+}/^{13}N^{7+}$ ratio	$(1.0 \pm 0.1) \times 10^{-5}$	$(1.5 \pm 0.2) \times 10^{-6}$
$^{13}\mathrm{C}_{\mathrm{g.s.}}$ $d\sigma/d\Omega(0°)$	17 ± 3 mb/sr	16 ± 3 mb/sr
$^{13}\mathrm{C}_{\mathrm{SE}}$ $d\sigma/d\Omega(0°)$	15 ± 3 mb/sr	22 ± 4 mb/sr
$^{13}\mathrm{C}_{\mathrm{DE}}$ $d\sigma/d\Omega(0°)$	44 ± 8 mb/sr	56 ± 10 mb/sr
σ_F^*	15 ± 2 mb/sr	13 ± 2 mb/sr
σ_{GT}^*	55 ± 10 mb/sr	74 ± 13 mb/sr
Other results[a]	$(^3\mathrm{He}, t)$ $E/A = 67$ MeV	(p, n) $E = 160$ MeV
σ_F^*	5.5 ± 0.5 mb/sr	1.6 ± 0.3 mb/sr
σ_{GT}^*	4.1 ± 0.2 mb/sr	4.2 ± 1.2 mb/sr

[a]References [12,13].

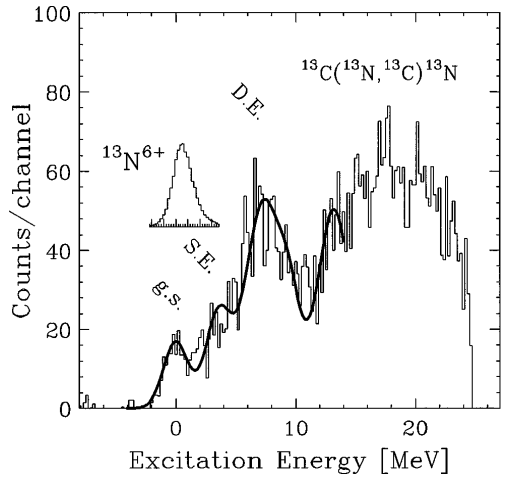

FIG. 2. Energy spectrum and fit for the ^{13}C(^{13}N,^{13}C)^{13}N reaction at $E/A = 105$ MeV. Higher excitations—one at 9.48 MeV—were also allowed in the fit to obtain a reliable measure of the DE cross section.

parity states in the 10–15 MeV region in the target residue, in combination with GT transitions to either the $1/2^-$ or the $3/2^-$ states in the ejectile as the only particle-stable negative-parity states in ^{13}C.

The present data were obtained with a spectrometer acceptance of approximately 3 msr, centered around 0°, and with significant sensitivity out to 4°, as shown by the solid line in Fig. 3. Since the secondary beam was too intense for counting individual ^{13}N ions at the reaction target, a compromise between beam rate and angular resolution was achieved by limiting the ^{13}N beam to an angular width of 10 mrad. The ^{13}N^{6+} angular distribution

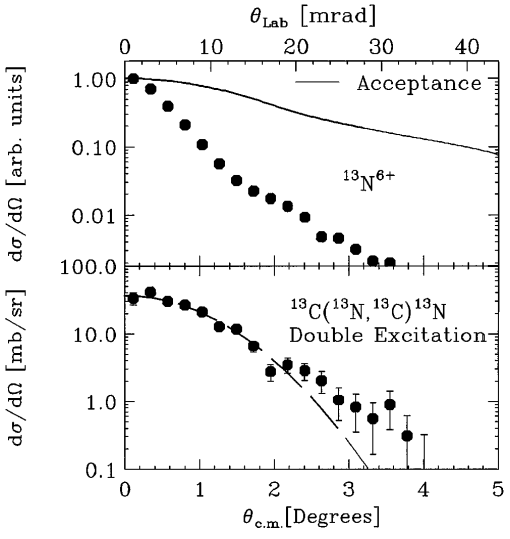

FIG. 3. Angular distribution for the ^{13}N^{6+} secondary-beam charge state and the $E/A = 105$ MeV ^{13}C(^{13}N,^{13}C)^{13}N DE reaction products, shown as an example. The experimental data have been corrected for acceptance, and the error bars represent statistical uncertainty only. The solid curve shows the spectrometer acceptance calculated with the computer code TURTLE [19]. The dashed curve is a Gaussian fit to the data, which is used in deconvoluting the secondary-beam resolution.

is shown in the top part of Fig. 3. In order to extract the forward cross section from the measured spectra, the angular width of the secondary beam had to be subtracted in quadrature from the (^{13}N,^{13}C) spectra. This correction was achieved by fitting the data with a Gaussian curve, which produced a satisfactory fit (see Fig. 3). In all cases, the cross section was found to be very forward peaked with widths (FWHM) of less than 3° and 2° in the center-of-mass system (c.m.) for the 57 and 105 MeV cases, respectively. The forward cross section $d\sigma/d\Omega(0°)$ was determined from the unfolded width and the peak area. The results are listed in Table I.

For (p,n) reactions, the relationship of zero-degree cross section to target transition strength is conventionally written [3] as

$$d\sigma/d\Omega(0°) = \hat{\sigma}_F F(q,\omega) B(F) + \hat{\sigma}_{\rm GT} F(q,\omega) B({\rm GT}), \quad (1)$$

where $\hat{\sigma}_F$ and $\hat{\sigma}_{\rm GT}$ are the cross sections per unit transition strength, and $F(q,\omega)$ is a function of momentum transfer, q, and energy loss, ω, which approaches unity as q and ω approach zero. $F(q,\omega)$ is estimated from systematics [3] to be greater than 0.95 (0.98) for the 57 MeV (105 MeV) experiment and will not be considered in the following. The empirical relationship for the ratio of the unit cross sections, used to calibrate (p,n) spectra at energies between 50 and 200 MeV, is $\hat{\sigma}_{\rm GT}/\hat{\sigma}_F = (E_p/55\ {\rm MeV})^2$ [3]. For HICEX, a more general form for the relationship between cross section and transition strength is needed:

$$d\sigma/d\Omega(0°) = \sigma^*_F B(F)_P B(F)_T + \sigma^*_{\rm GT} B({\rm GT})_P B({\rm GT})_T, \quad (2)$$

where the transition strengths in both projectile (P) and target (T) are taken into account, and σ^* replaces $\hat{\sigma}$. The latter is only defined for the (p,n) reaction, where $\sigma^*_F = \hat{\sigma}_F$ and $\sigma^*_{\rm GT} = \frac{1}{3}\hat{\sigma}_{\rm GT}$, since $B(F) = 1$ and $B({\rm GT}) = 3$. The structural symmetry of the mirror nuclei allows us to write

$$d\sigma/d\Omega(0°)_{\rm g.s.} = \sigma^*_F B(F)^2_{1/2^-} + \sigma^*_{\rm GT} B({\rm GT})^2_{1/2^-}, \quad (3)$$

$$d\sigma/d\Omega(0°)_{\rm SE} = 2\sigma^*_{\rm GT} B({\rm GT})_{1/2^-} B({\rm GT})_{3/2^-}, \quad (4)$$

$$d\sigma/d\Omega(0°)_{\rm DE} = \sigma^*_{\rm GT} B({\rm GT})^2_{3/2^-}. \quad (5)$$

There is no mixing of Fermi and GT-type transitions, since the interaction is one step in nature. Using our measured cross sections, $B(F)_{1/2^-} = 1$, and the literature values $B({\rm GT})_{1/2^-} = 0.200 \pm 0.004$ (from β decay) and $B({\rm GT})_{3/2^-} = 0.83 \pm 0.03$ [from the (p,n) reaction] [12], we can solve for σ^*_F and $\sigma^*_{\rm GT}$. The results are given in Table I. For comparison, we have included experimental results obtained for ^{13}C targets with beams of protons and ^{3}He [12,13]. The specific cross sections found for the present case are surprisingly large, and $\sigma^*_{\rm GT}$ shows a small increase with increasing energy, while σ^*_F decreases slightly. This is in contrast with (p,n) charge exchange, where $\sigma^*_{\rm GT}$ remains unchanged, while σ^*_F decreases with energy [3]. In ^{12}C(^{12}C,^{12}N)^{12}B HICEX, however, an

increase in GT cross section has been observed, with values for $\sigma^*_{\rm GT}$ of 5.4 mb/sr (17 mb/sr) at $E/A = 70$ MeV (135 MeV) [5,6]. The increase in cross section is attributed to enhanced transparency of the nucleus at higher energy [6]. A test of proportionality that is independent of calibration is obtained by combining Eqs. (4) and (5),

$$\frac{d\sigma/d\Omega(0°)_{\rm DE}}{d\sigma/d\Omega(0°)_{\rm SE}} = \frac{B({\rm GT})_{3/2^-}}{2\,B({\rm GT})_{1/2^-}}\,. \qquad (6)$$

The experimentally obtained values for the left-hand side of Eq. (6) are 2.9 ± 0.5 (2.5 ± 0.7) for the 57 MeV (105 MeV) experiment, in fair agreement with the right-hand-side value of 2.08 ± 0.09. A model calculation [14] for the ^{13}C(^{13}N,^{13}C)^{13}N reaction at $E/A = 70$ MeV predicts 3.5 mb/sr for the GT part of the forward g.s. cross section. The experimental value, determined from Eq. (3), is 2.2 ± 0.4 mb/sr.

For further comparison, the values of $\sigma^*_{\rm GT}/\sigma^*_F$ as a function of energy for the three charge-exchange reactions ^{13}C$(p,n)^{13}$N [3,12,15], ^{13}C$(^3$He$,t)^{13}$N [13,16], and ^{13}C(^{13}N,^{13}C)^{13}N are shown in Fig. 4. The data indicate that $\sigma^*_{\rm GT}/\sigma^*_F$ increases with projectile mass. We attribute this increase to the strong absorption in heavy-ion reactions, which selects large impact parameters and therefore emphasizes the longest-range part of the nuclear force. The spin-flip part of the interaction is mediated by single-pion exchange and hence is enhanced with respect to the non-spin-flip portion, which has the shorter-range characteristics of multiple-pion exchange.

There is a controversy regarding the relationship between (p,n) cross section and GT strength in ^{13}C. The observed cross section for the $3/2^-$ state was found to be small compared to the shell-model B(GT) value beyond the well-known GT quenching [12,17]. Some authors [18] contend that the procedure used to calibrate the unit cross section $\hat{\sigma}_{\rm GT}$ in the former work is faulty and that it is the $1/2^- - 1/2^-$ GT transition that has an anomalous cross section. We have used the results of Ref. [12] in the present paper, since it represents the conventional approach, and the issue remains unresolved at the present time.

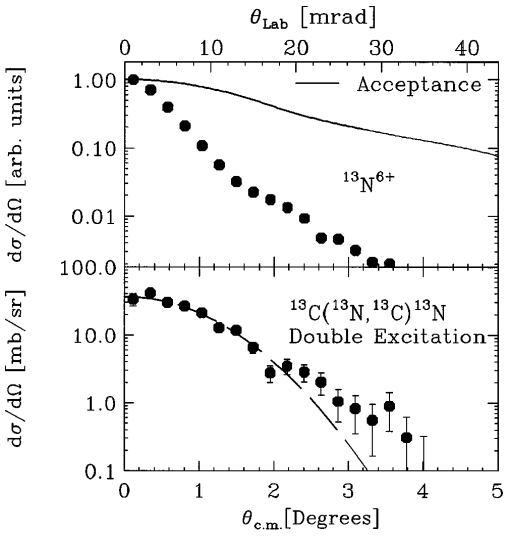

FIG. 4. Energy dependence of $\sigma^*_{\rm GT}/\sigma^*_F$ for a number of charge-exchange reactions performed on ^{13}C targets. The dotted line is the equivalent of the $\hat{\sigma}_{\rm GT}/\hat{\sigma}_F = [E_p/(55\ {\rm MeV})]^2$ curve, scaled appropriately.

In conclusion, we have measured the 0° cross sections for the three lowest excitations of the ^{13}C(^{13}N,^{13}C)^{13}N reaction in the first mirror charge-exchange experiment. The structure of the excitation spectrum permits a simple interpretation in terms of weak-interaction strengths, and the symmetry of the mirror pair was exploited to determine the cross sections per unit transition strength. The ratio of the Gamow-Teller unit cross section to the Fermi unit cross section was found to be several times larger than for the (p,n) charge exchange. The present results are encouraging and indicate that HICEX could become a powerful tool for measurements of GT strengths in radioactive nuclei.

We thank G. F. Bertsch for suggesting this project. This research was supported by the National Science Foundation under Grant No. PHY-92-14922.

*Present address: Instituto de Fisica, Universidade Federal do Rio de Janeiro, C. Postal 68528, 21945-970 Rio de Janeiro, RJ, Brazil.
†Present address: GSI, Postfach 110552, D-64220 Darmstadt, Germany.
‡Present address: Cyclotron Laboratory, RIKEN, 2-1 Hirosawa, Wako, Saitama 351-01, Japan.
§Present address: LPC, IN2P3-CNRS, ISMRA et Université de Caen, 14050 Caen Cedex, France.
‖Present address: Cyclotron Institute, Texas A & M University, College Station, TX 77843.
¶Present address: Department of Physics, Yale University, New Haven, CT 06511.

[1] M. B. Aufderheide *et al.*, Phys. Rev. C **48**, 1677 (1993).
[2] C. D. Goodman *et al.*, Phys. Rev. Lett. **44**, 1755 (1980).
[3] T. N. Taddeucci *et al.*, Nucl. Phys. **A469**, 125 (1987).
[4] J. S. Winfield *et al.*, Phys. Rev. C **35**, 1734 (1987).
[5] N. Anantaraman *et al.*, Phys. Rev. C **44**, 398 (1991).
[6] T. Ichihara *et al.*, Phys. Lett. B **323**, 278 (1994).
[7] H. Lenske, H. H. Wolter, and H. G. Bohlen, Phys. Rev. Lett. **62**, 1457 (1989).
[8] F. Osterfeld *et al.*, Phys. Rev. C **45**, 2854 (1992).
[9] D. T. Khoa, W. von Oertzen, and H. G. Bohlen, Phys. Rev. C **49**, 1652 (1994).
[10] B. M. Sherrill *et al.*, Nucl. Instrum. Methods Phys. Res., Sect. B **56**, 1106 (1991).
[11] W.-T. Chou, B. A. Brown, and E. K. Warburton, Phys. Rev. C **47**, 163 (1993).
[12] J. Rapaport *et al.*, Phys. Rev. C **36**, 500 (1987).
[13] J. Jänecke *et al.*, Nucl. Phys. **A526**, 1 (1991).
[14] C. A. Bertulani, Nucl. Phys. **A554**, 493 (1993).
[15] J. Rapaport (private communication).
[16] H. Akimune *et al.*, Nucl. Phys. **A569**, 245c (1994).
[17] C. D. Goodman *et al.*, Phys. Rev. Lett. **54**, 877 (1985).
[18] J. W. Watson *et al.*, Phys. Rev. Lett. **55**, 1369 (1985).
[19] D. C. Carey, National Accelerator Laboratory Report No. NAL-64.2041, 1964.